Fragility analysis of bridge pier supported on rocking shallow foundation under earthquake loading

B. S. Deviprasad[1] · Ramanandan Saseendran[1] · G. R. Dodagoudar[1]

Abstract

The rocking shallow foundation (RSF) allows seismic protection of the superstructure by guiding the plastic hinge onto the soil. Fragility curves are probabilistic measures to estimate the likelihood that a structure and/or its components exceed a particular damage state for a given intensity measure. In this study, the fragility analysis of the bridge pier-RSF system is carried out to quantify the seismic damage in a probabilistic framework. The deterministic finite element model of the bridge pier-RSF system is created using BNWF modelling approach and is implemented in OpenSees platform. Five broadband and five pulse-type ground motions are selected from the PEER ground motion database and are modified to generate sixty more ground motions for the response analysis of the system. The probabilities of failure are evaluated using the Monte Carlo simulation technique considering four engineering design parameters, four model configurations and seventy ground motions for the three performance levels. Results of the analyses showed that the bridge pier-RSF system is more vulnerable in the case of pulse-type ground motions compared to the broadband-type. This study is an initial attempt to develop the fragility curves which will be helpful in the seismic vulnerability assessment of the bridge pier-RSF systems.

✉ B. S. Deviprasad
  deviprasad.bsg@gmail.com

  Ramanandan Saseendran
  ramanandans@gmail.com

  G. R. Dodagoudar
  goudar@iitm.ac.in

[1] Department of Civil Engineering, Indian Institute of Technology Madras, 600036 Chennai,

1 Introduction

In the case of bridges supported on conventional fixed-base (FB) foundations, the dissipation of seismic energy occurs by formation of plastic hinges in the bridge pier (CALTRANS 2016). Even if the FB bridges do not collapse during earthquakes, the bridge system may experience considerable plastic deformations necessitating repair and partial or perhaps even the complete demolition (Herdrich 2015). Hence, as an alternate design approach, the bridge pier can be supported on rocking shallow foundation (RSF). The plastic hinges are guided onto the soil in this case by allowing the foundation to rock and uplift. Thus, the inevitable nonlinear failure mechanisms of the soil can be used for the seismic protection of the superstructure (Paolucci 1997; Pecker 2003; Kutter et al. 2006; Gerolymos et al. 2008; Anastasopoulos et al. 2010). The seismic performance of the bridges supported on the RSF have been analyzed deterministically by many researchers and it was reported that the bridges undergo larger settlements compared to the FB bridges but suffer less damage due to smaller residual drift during the earthquake loading (Anastasopoulos et al. 2010; Antonellis 2015; Deviprasad and Dodagoudar 2020).

The deterministic studies do not consider the uncertainties associated with soil and structural parameters. However, it is necessary to consider the uncertainties in order to evaluate the seismic vulnerability of the bridge system realistically. The fragility curves are used to define and quantify the seismic damage in a probabilistic framework. The fragility curve is a probabilistic measure representing the probability of exceeding a given damage state as a function of an engineering design parameter (EDP) that represents the response of a structure due to ground motion of a particular intensity level. The different approaches used to develop the fragility curves are (i) based on expert opinion, (ii) empirical methods, (iii) analytical methods and (iv) numerical methods. The method based on the expert opinion is completely subjective in nature. The empirical fragility curves are based on observational data and have limited application as they are related to a specific earthquake and a structure (Jeong and Elnashi 2007). Analytical fragility curves are based on structural models that characterize the performance limit states of the structure. These are very useful, where earthquake data is limited or not available. However, it is difficult to obtain a closed form solution for the probability of failure with respect to the different limit states of the system. The limitations of the above methods of developing the fragility curves can be overcome by the numerical method. The fragility curves developed by the numerical method are based on numerical simulation of the seismic performance of the structures. A number of studies have been reported for bridges using the above-mentioned approaches (Shinozuka et al. 2000; Hwang et al. 2000; Kim and Feng 2003; Elnashi et al. 2004; Mackie and Stojadinovic 2005; Nielson 2005; Jeong and Elnashi 2007; Ni et al. 2018). However, all the fragility curves are developed for the bridges supported on FB foundations.

In this study, the fragility analysis of the bridge-pier RSF system is carried out using Monte Carlo simulation (MCS) technique with Latin hypercube sampling (LHS). The deterministic finite element (FE) model of the bridge-pier RSF system is modelled using beam on nonlinear Winkler foundation (BNWF) approach in OpenSees platform. The ground motions for the response analysis are selected from the PEER ground motion database compatible with the target spectrum as per IS 1893 (Part 1): 2016 for Zone IV and Type II soil. The fragility curves are developed for three performance levels: immediate occupancy (IO), life safety (LS), and collapse prevention (CP) considering the peak ground acceleration

(PGA) as the intensity measure. The beneficial effects of the RSF in the response analysis of the bridge pier-RSF system are assessed considering the broadband-type and pulse-type ground motions.

2 Methodology

The methodology adopted for the fragility analysis of the bridge pier-RSF system is presented in this section. The methodology is depicted pictorially in Fig. 1. The initial step is selection and scaling of the ground motions. Once a ground motion suite is generated, that is considered as input to the different model configurations and responses of interest are evaluated. The probabilities of failure are then evaluated and plotted with the PGA for all the combinations of the model configurations, EDPs and ground motion types. The detailed explanation of the methodology is given in subsequent sections.

2.1 Finite element Model and Model Configurations

The bridge pier-RSF system is considered as resting on the homogenous medium dense to dense sand strata. The geometrical properties of the model and material properties of the soil are given in Tables 1 and 2, respectively. Four model configurations corresponding to the height of the pier (H_c) to the width of foundation (B_f), i.e., H_c/B_f ratios of 1.5, 2.0, 2.5 and 3.0 are considered to understand the influence of footing width on the seismic performance of the system. The Young's modulus of concrete (E_c) is taken as 27 GPa. The total seismic weight is taken as 15 MN for all the four configurations. The sensitivity analysis was performed using 2^k factorial design to identify the most influential parameters on the response of the bridge pier-RSF system and are published elsewhere (Deviprasad et al. 2021). It has been concluded that the maximum bending moment of the footing (*MBM*) and residual ver-
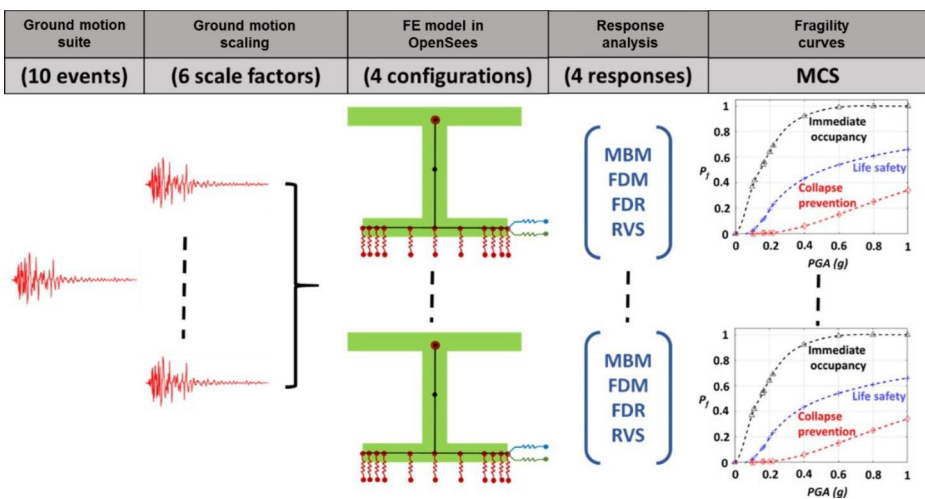

Fig. 1 Methodology of fragility analysis for bridge pier-RSF system

Table 1 Geometrical characteristics of the bridge pier-RSF system

Bridge deck	Width, B_{deck} (m)	12.2
	Length, L_{deck} (m)	12.2
	Height, H_{deck} (m)	1.8
Bridge pier	Height, H_c (m)	12.2
	Diameter, D_c (m)	2
Foundation	H_c/B_f ratio	1.5, 2, 2.5, 3
	Height, H_f (m)	1.8
	Embedment depth, D_f (m)	2.4

Table 2 Material properties of the soil

Soil type	Young's modulus, E_s (MN/m^2)	Poisson's ratio, v	Friction angle, ϕ (°)	Unit weight, γ_s (kN/m^3)	Damping ratio, ξ_s (%)
Sand (medium dense to dense)	40 (30 to 50)	0.3	36 (30 to 42)	18 (15.3 to 20.7)	5 (2.5 to 7.5)
Coefficient of variation (%)	15	-	10	9	30

tical settlement of the footing (*RVS*) are sensitive to the uncertainties in the angle of internal friction (ϕ), Young's modulus (E_s), and unit weight (γ_s) of the soil. The horizontal displacement due to flexure alone, in addition to the above-mentioned three parameters, is found to be sensitive to the damping ratio of the soil (ξ_s) as well. Hence, in the present study, the uncertainties with respect to the above-mentioned parameters are considered for the fragility analysis with respect to the three performance levels. The upper level and lower level of the random variables considered (Table 2) are $\mu + 1.65\sigma$ and $\mu - 1.65\sigma$ respectively, where μ is the mean and σ is the standard deviation of the respective variable. In Table 2, the values inside the brackets represent the lower and upper levels of the respective random variables and the values outside the bracket represent the mean values. All the random variables are considered as normally distributed in the analysis. Therefore, the range between the upper and lower levels include 90% of the uncertainties in the random variables.

The deterministic behavior of the RSF is modelled using the BNWF approach in OpenSees platform. A number of studies have been reported on the use of BNWF model for the performance analysis geotechnical structures (e.g., Raychowdhury 2008; Gerolymos et al. 2009; Antonellis 2015; Pelekis et al. 2021). Figure 2 shows the schematic of the BNWF model for the bridge pier-RSF system. The approach based on the BNWF model consists of elastic beam-column elements to capture the structural (footing and pier) behavior and zero-length elements to model the soil-footing interaction. The zero-length elements, viz. q-z, p-x and t-x springs (Fig. 2) are incorporated to capture the vertical load-displacement, horizontal passive load-displacement and shear-sliding behavior, respectively. The gap elements added in series with the elastic and plastic elements account for soil-foundation separation. The zero-length element springs are characterized by the nonlinear backbone curves which are bilinear in nature with linear and nonlinear regions representing the degrading stiffness as the displacement increases. The material models available for the zero-length elements in OpenSees library (Boulanger et al. 1999; Boulanger 2000) are for the pile foundations whose backbone curves are calibrated against the pile load tests. For shallow foundations,
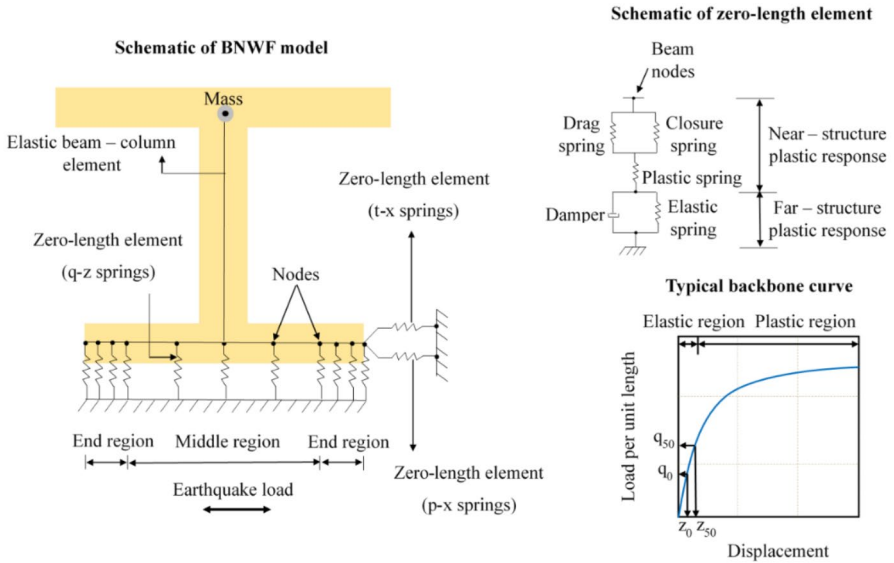
Fig. 2 Schematic of the BNWF model for bridge pier-RSF system

the modified versions of the above curves (Raychowdhury 2008) are used which are calibrated with the results of the load tests on shallow foundations. Detailed explanations of the finite element modelling including the description of the material model and validation studies are given elsewhere (Deviprasad and Dodagoudar 2020) and the same is not repeated here.

2.2 Engineering Design Parameters and Limit States

The reservations to adapt the RSF in bridges as an alternative to the FB foundations can be attributed to (i) the general notion that the strength of the RSF is uncertain, (ii) concerns regarding the overturning of bridges due to rocking and (iii) lack of comprehensive approaches to evaluate the drift and settlements of the bridge-RSF system (Deng et al. 2012). The concern regarding the uncertainty of strength of the RSF and the lack of procedure for evaluating the drift and settlements is addressed by considering the maximum and residual horizontal displacements of the deck due to flexure alone (*FDM* and *FDR* respectively) and *RVS* as the three EDPs in the study. In case of bridges on RSF, the deck drift has two components: (i) drift due to flexural distortion of the bridge pier and (ii) drift due to rocking motion of the footing. The flexural drift causes permanent or plastic deformation of the bridge pier. This is another reason why the flexural drift is considered as one of the critical performance criteria to assess the seismic performance. The bridge pier overturns when the moment capacity of the RSF is exceeded. Therefore, to address the concern regarding the overturning due to rocking, the *MBM* is considered as the fourth EDP.

The methodology of deterministic analysis of the bridges on RSFs is well established and is similar to that of the conventional shallow foundations. However, the use of RSFs for bridges is not still common in practice. Therefore, the limit states or threshold values for dif-

ferent responses are not readily available in the literature and are chosen in this study based on the guidelines available for the conventional bridge design and other related structures. The threshold values for the *MBM* are expressed in terms of rocking moment capacity of the footing (Deng and Kutter 2012) whereas, for the *FDM*, *FDR* and *RVS* are selected appropriately based on the published results (Bozozuk 1978; FEMA-356; Eurocode 8; Yakut and Solmaz 2012). In the study, the limit states for the EDPs are defined considering three performance levels, viz. immediate occupancy (IO) corresponding to slight damage, life safety (LS) corresponding to moderate overall damage and collapse prevention (CP) corresponding to severe structural damage. The corresponding threshold or limiting values for all the EDPs and performance levels are listed in Table 3.

2.3 Selection and scaling of Ground Motions

As per IS 1893 (Part 1): 2016, the minimum number of ground motions required for the time history analysis of the structure are seven. In this study, ten ground motions corresponding to five broadband-type and five pulse-type events are selected considering a few earthquake

Table 3 Threshold values for the four responses of the bridge pier-RSF system

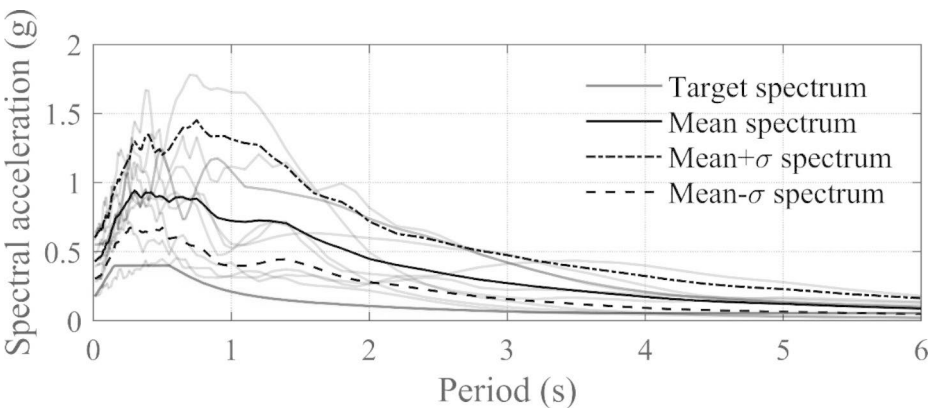| Response	Performance level	Threshold values			
		$H_c/B_f = 1.5$	$H_c/B_f = 2.0$	$H_c/B_f = 2.5$	$H_c/B_f = 3.0$
MBM (kNm)	IO	12,500	10,000	7500	6250
	LS	25,000	20,000	15,000	12,500
	CP	50,000	40,000	30,000	25,000
FDM and *FDR* (mm)	IO	25			
	LS	100			
	CP	150			
RVS (mm)	IO	25			
	LS	50			
	CP	100			

Fig. 3 Target and mean spectra and response spectra of the selected unscaled ground motions

characteristics such as magnitude, rupture distance and fault mechanism from the PEER strong motion database. The ground motions are selected in such a way that, their mean response spectrum is compatible with the target spectrum as per IS 1893 (Part 1): 2016 corresponding to Zone IV and Type II soil (Fig. 3). The acceleration time histories selected correspond to recording stations with medium-stiff to stiff soil site conditions (Average shear wave velocity up to 30 m depth, V_{s30} = 180 to 360 m/s). The characteristics of the selected horizontal ground motions are given in Table 4. The amplitudes of the ground motions are

Table 4 Characteristics of acceleration time histories of the selected ground motions

| Earthquake Type	Name	Year	Station name	Faulting type	Rupture distance (km)	M_w	Vs_{30} (m/s)	PGA (g)
Broadband	Imperial valley	1979	Parachute test site	Strike slip	12.69	6.53	348.69	0.11
	Loma Prieta	1989	Coyote lake dam (downstream)	Reverse oblique	20.8	6.93	295.01	0.16
	Northridge	1994	LA-W 15th S	Reverse	29.74	6.69	329.52	0.098
	Kobe	1995	Abeno	Strike slip	24.85	6.9	256	0.22
	Darfield	2010	RKAC	Strike slip	16.47	7	295.74	0.17
Pulse	Imperial valley	1979	Meloland Geot. Array	Strike slip	0.07	6.53	264.57	0.3
	Superstition hills	1987	Parachute test site	Strike slip	0.95	6.54	348.69	0.38
	Northridge	1994	Newhall- W Pico canyon road	Reverse	5.48	6.69	285.93	0.357
	Kocaeli	1999	Yarimca	Strike slip	4.83	7.51	297	0.32
	Chi-Chi	1999	TCU051	Reverse oblique	7.64	7.62	350.06	0.24
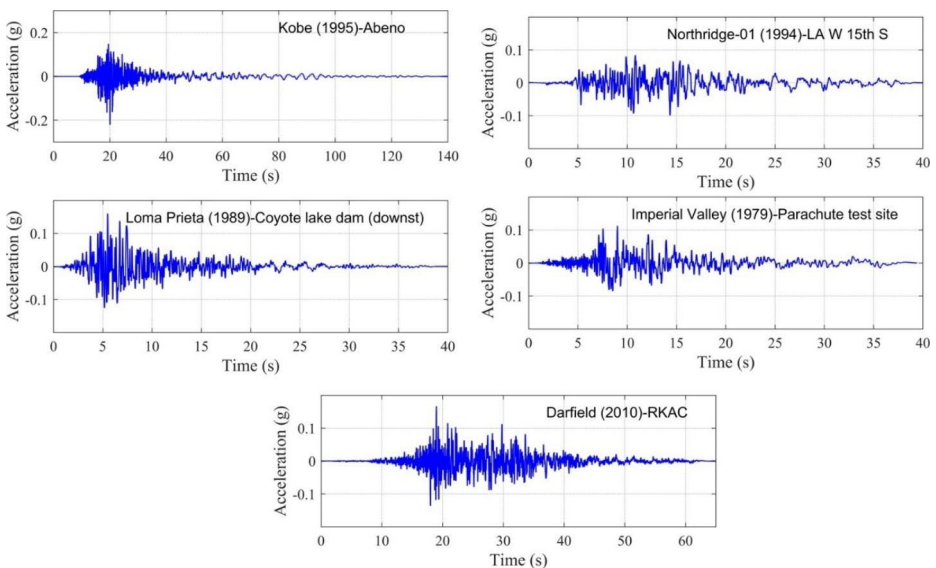
Fig. 4 Time histories of the selected broadband-type ground motions

modified appropriately to generate similar acceleration time histories. The ground motions are scaled to PGA values of 0.1 g, 0.2 g, 0.4 g, 0.6 g, 0.8 and 1 g to represent all the damage states of the bridge pier-RSF system. From the one unscaled ground motion, six more scaled records are obtained and are used in the assessment of the seismic response. The time histories of the unscaled broadband-type and pulse-type motions are shown in Figs. 4 and 5 respectively.

2.4 Probability of failure and Monte Carlo Simulation technique

The safety and serviceability of the structure is assessed using probabilistic methods by evaluating the probability of failure (P_f). If Q is the resistance or capacity of the structure and S is the demand on the structure, then the failure is expressed as

$$f = Q - S < 0 \tag{1}$$

The failure, f is a function of several demand and capacity variables which can be expressed as

$$f(X_1, X_2, \ldots, X_k) = f(\boldsymbol{X}) \tag{2}$$

where $\boldsymbol{X}$ is the k-dimensional vector of random variables X_1, X_2, ..., X_k, related to different capacity and demand variables. The limit state $f(X)=0$ is the boundary between the safe domain [$f(X)>0$] and the failure domain [$f(X)<0$]. Then the P_f is expressed as
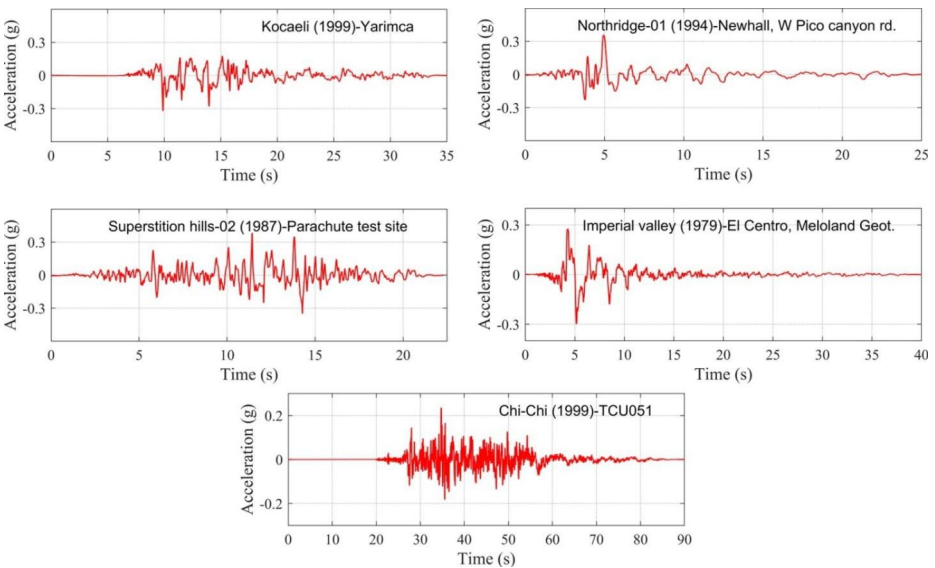
$$P_f = P[f(\boldsymbol{X}) < 0] \tag{3}$$

Fig. 5 Time histories of the selected pulse-type ground motions

If Q and S are correlated and $f_{QS}(q, s)$ is the joint probability density function of Q and S, the P_f is expressed as

$$P_f = \iint_{f(\mathbf{X})<0} f_{QS}(q, s) \, dq \, ds \tag{4}$$

It is difficult to obtain the closed form solution for the above equation and hence, alternate solution methods are required for the evaluation of P_f. In the case of responses evaluated using the finite element method, a simulation technique like the MCS is more appropriate to evaluate the associated P_f. In recent times, the MCS technique has been used extensively in geotechnical and structural engineering (e.g., Radu and Grigoriu 2018; Díaz et al. 2018; Liu and Change 2020; Ni et al. 2020; Giordano et al. 2021). In the present study, the probabilities of failure needed for the construction of the fragility curves are evaluated using the direct application of the MCS technique, wherein the FE analyses are carried out for n number of realizations of the bridge pier-RSF system corresponding to n number of realizations of the different random variables set, sampled according to their respective probabilistic characteristics. If n_f is the number of times the threshold values are exceeded out of the n realizations, the probability of failure is expressed as

$$P_f = \frac{n_f}{n} \tag{5}$$

The MCS technique requires a sampling scheme which can represent the variability and range of a particular random variable. In the case of random sampling, new sample points are generated without considering the previously generated sample points. This may lead to the consideration of only localized randomness within the range of values for a random variable. Hence, the Latin hypercube sampling (LHS) technique is adopted in the study for generating random values of the input uncertain parameters considering their associated uncertainties. The LHS method equally divides the uncertainty range of a random variable into a specified number of intervals and selects a random value from each interval for the random variable under consideration. The LHS ensures that the random sampling is representative of the uncertainty of the variable. In addition, the LHS also reduces the computer processing time as it optimizes the number of simulations. The number of simulations required in the MCS technique using the LHS is determined by comparing the maximum change in the P_f observed for different number of trial runs (Table 5). Figure 6 shows the variation of the P_f corresponding to the *MBM* and *RVS* with respect to the number of real-

Table 5 Number of simulations and corresponding maximum change in P_f values

Simulation number	Maximum change in P_f (%)
10 to 100	≈ 38
100 to 1000	≈ 13
1000 to 5000	1.3
5000 to 10,000	0.8
10,000 to 100,000	0.8

Fig. 6 Variation of P_f for *MBM* and *RVS* with number of simulations
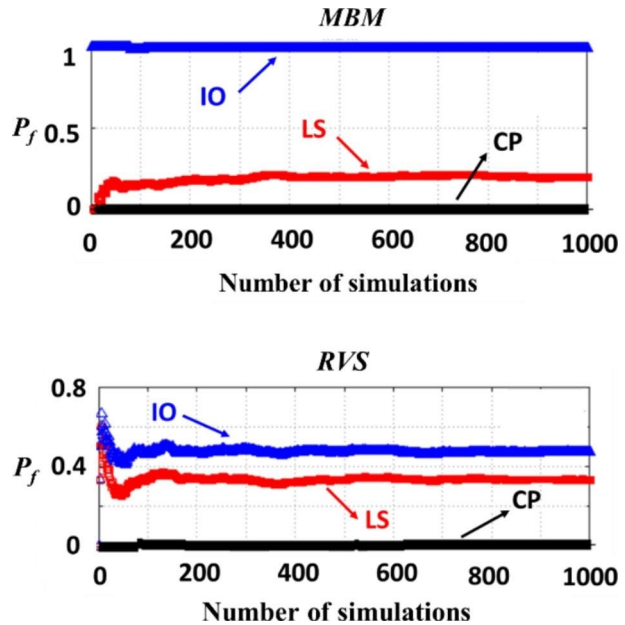
izations. It is observed that one thousand number of simulations ensure a stable P_f value beyond which the change in the P_f is negligible.

3 Results and discussion

The probabilities of exceedance corresponding to the four EDPs (i.e., *MBM, FDM, FDR* and *RVS*) for different seismic intensities (i.e., PGA values) and for all the model configurations are evaluated using the MCS and are plotted as the fragility curves in Figs. 7, 8, 9, 10, 11, 12, 13 and 14. Figures 7, 8, 9 and 10 depict the fragility curves for H_c/B_f ratios of 1.5, 2, 2.5, and 3 for the broadband-type ground motions and Figs. 11, 12, 13 and 14 depict the fragility curves for the pulse-type ground motions. In Figs. 7, 8, 9, 10, 11, 12, 13 and 14, the FDM_a, FDR_a, $M_{c\,foot}$ and RVS_a are the threshold values for the *FDM, FDR, MBM* and *RVS* respectively. The fragility curves quantify the seismic damage associated with the IO, LS, and CP performance levels and are the main performance indicators of the performance-based design in earthquake engineering. Using these curves, the component level damage state of the bridge pier-RSF system can be assessed for the future earthquakes. The P_f values corresponding to different intensities are useful for assessing the expected loss that a particular bridge pier-RSF system may undergo in the future earthquakes.

It is observed from the figures that the P_f values for the *FDM, FDR* and *MBM* reduce with increase in the H_c/B_f ratio but the P_f for the RVS increases with increase in the H_c/B_f ratio. This can be attributed to the increased rocking because of the decreasing width of the foundation. The rocking effect is higher when the H_c/B_f ratio is 3, which results in the higher reliability with respect to the limit states corresponding to the *FDM, FDR* and *MBM*. However, for the case when the H_c/B_f ratio is 1.5, the rocking effect is lesser and consequently the lesser reliability with respect to the said limit states. Moreover, the IO
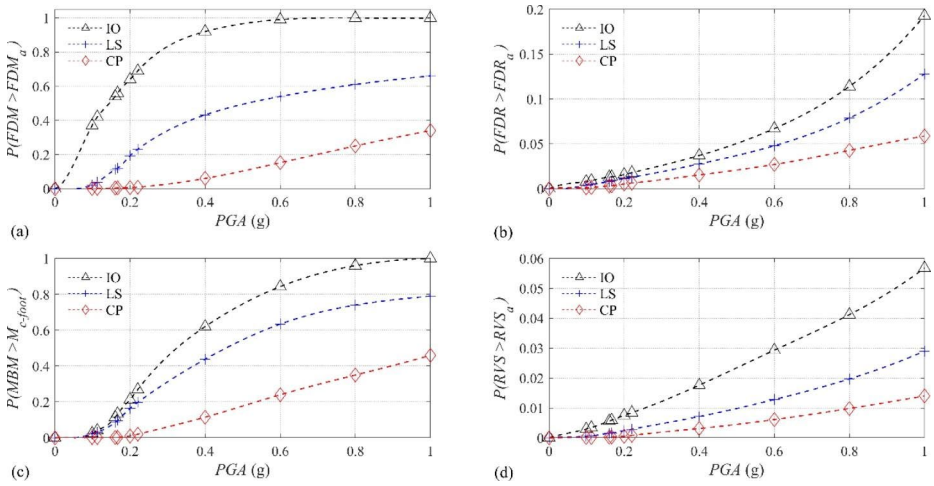
Fig. 7 Fragility curves for bridge pier with RSF corresponding to $H_c/B_f = 1.5$ for four EDPs and broadband-type earthquakes: (a) *FDM*; (b) *FDR*; (c) *MBM*; and (d) *RVS*
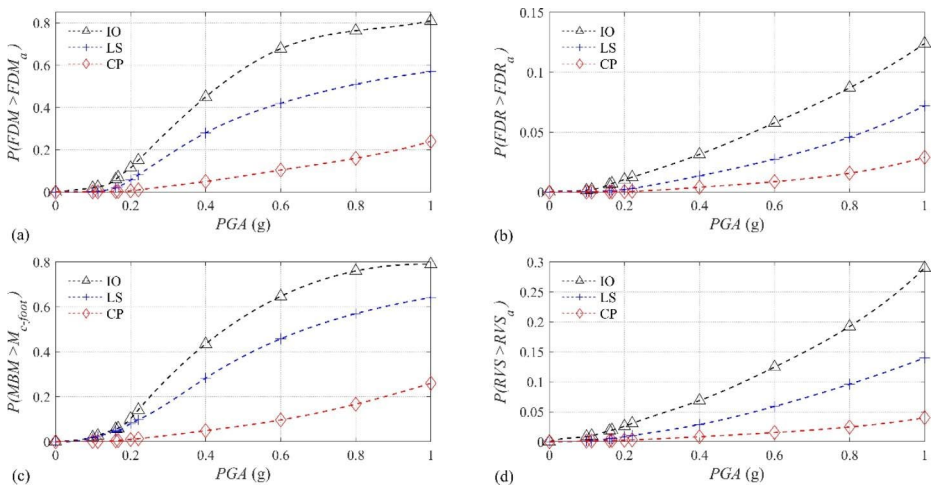

Fig. 8 Fragility curves for bridge pier with RSF corresponding to $H_c/B_f = 2.0$ for four EDPs and broadband-type earthquakes: (a) *FDM*; (b) *FDR*; (c) *MBM*; and (d) *RVS*

performance level has the highest variation in the probabilities of exceedance with the H_c/B_f ratio and the CP performance level has the lowest irrespective of the limit states considered. For the LS performance level, the probability of exceedance falls in between the above two performance levels. It is also observed that the probabilities of exceedance for the different responses (*FDM*, *FDR*, *MBM* and *RVS*) vary with the H_c/B_f ratios for all the performance levels. This leads to the conclusion that, the reliability of the bridge pier-RSF system is not uniform across the different H_c/B_f ratios. Hence, a careful dimensioning of the RSF for the bridges should be made without compromising the safety and serviceability of the system. It
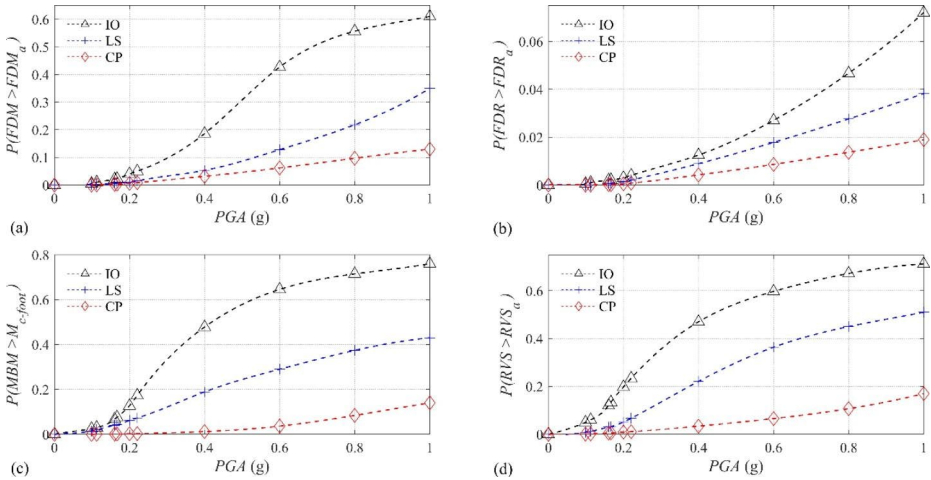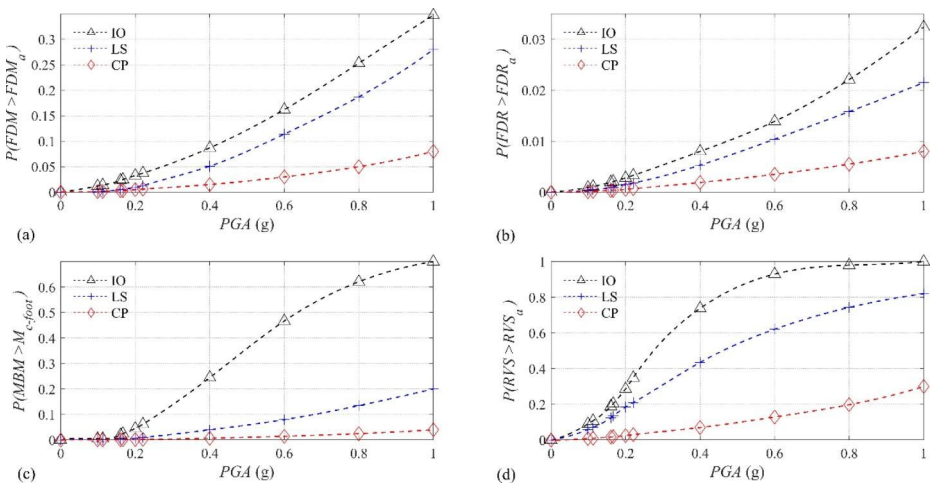
Fig. 9 Fragility curves for bridge pier with RSF corresponding to $H_c/B_f = 2.5$ for four EDPs and broadband-type earthquakes: (a) *FDM*; (b) *FDR*; (c) *MBM*; and (d) *RVS*

Fig. 10 Fragility curves for bridge pier with RSF corresponding to $H_c/B_f = 3.0$ for four EDPs and broadband-type earthquakes: (a) *FDM*; (b) *FDR*; (c) *MBM*; and (d) *RVS*

is advocated to define the performance criteria as a combination of the maximum allowable probability of failure and the corresponding performance levels.

Figure 15 shows the fragility curves for the broadband (BB) and pulse-type (P) ground motions for all the EDPs corresponding to the LS performance level of the bridge pier-RSF system with $H_c/B_f = 2.5$. It is seen that the P_f values corresponding to the *MBM* and *FDM* are higher for the pulse-type motions compared to the broadband-type motions. However, the P_f values corresponding to the *RVS* are lower for the pulse-type motions compared to the broadband-type motions. This could be attributed to the shorter duration of the higher amplitudes of the pulse-type motions. According to Newton's second law of motion, the
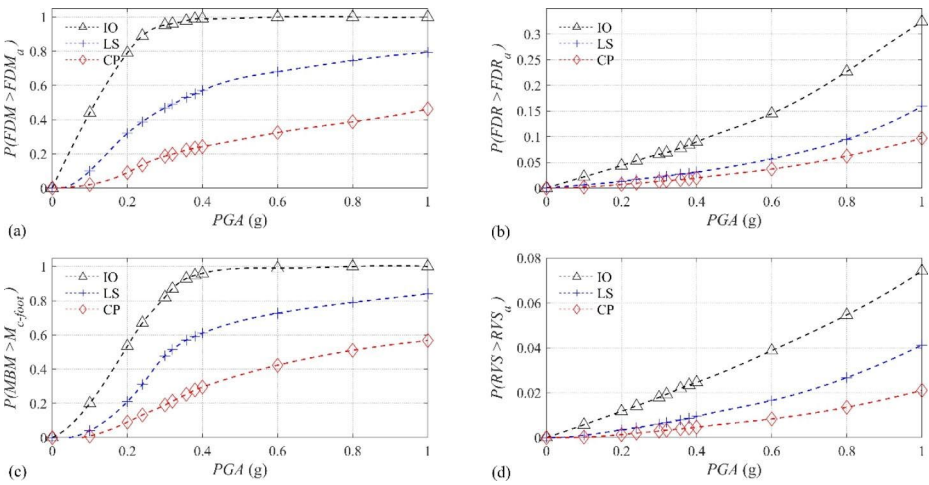
Fig. 11 Fragility curves for bridge pier with RSF corresponding to $H_c/B_f = 1.5$ for four EDPs and pulse-type earthquakes: (a) *FDM*; (b) *FDR*; (c) *MBM*; and (d) *RVS*
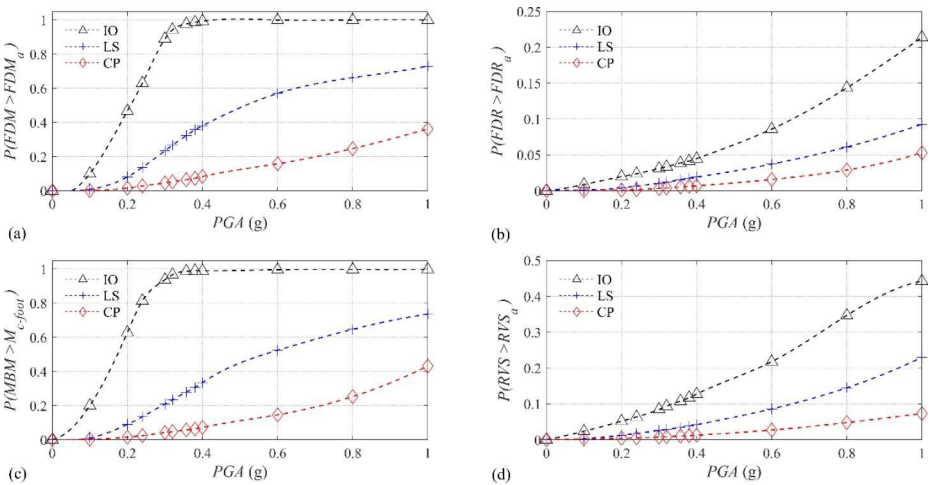

Fig. 12 Fragility curves for bridge pier with RSF corresponding to $H_c/B_f = 2.0$ for four EDPs and pulse-type earthquakes: (a) *FDM*; (b) *FDR*; (c) *MBM*; and (d) *RVS*

time rate of change of momentum is directly proportional to the force applied on the body. This implies that the pulse-type motions impart higher rate of change of momentum hence the higher magnitude of force is applied to the bridge pier-RSF system. In addition, as the duration of the higher amplitude motion is very short in the case of pulse-type motions, the complete mobilization of the soil strength does not take place. This results in reduced rocking of the foundation. As observed earlier, because of the lesser rocking effect, the *MBM* and *FDM* are higher and the *RVS* is lower. However, the beneficial effects of the rocking of the foundation are still significant during the pulse-type ground motions. The difference in
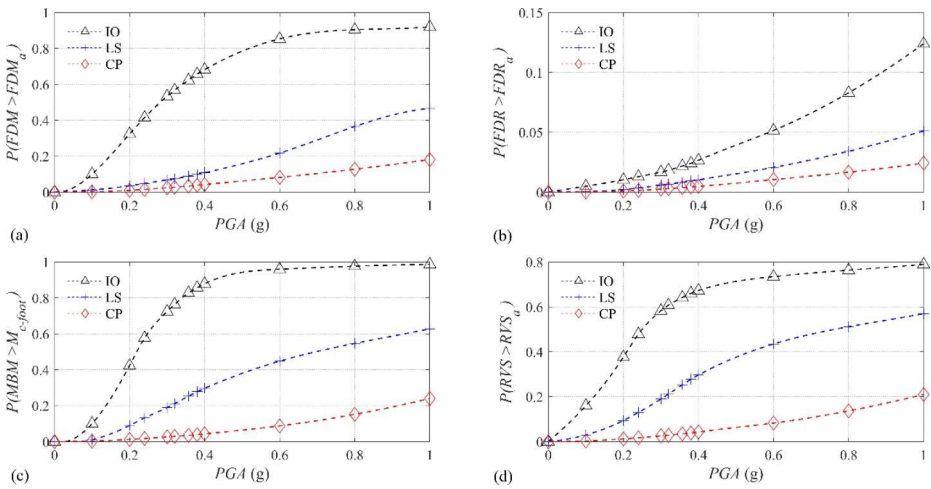
Fig. 13 Fragility curves for bridge pier with RSF corresponding to H_c/B_f =2.5 for four EDPs and pulse-type earthquakes: (a) *FDM*; (b) *FDR*; (c) *MBM*; and (d) *RVS*
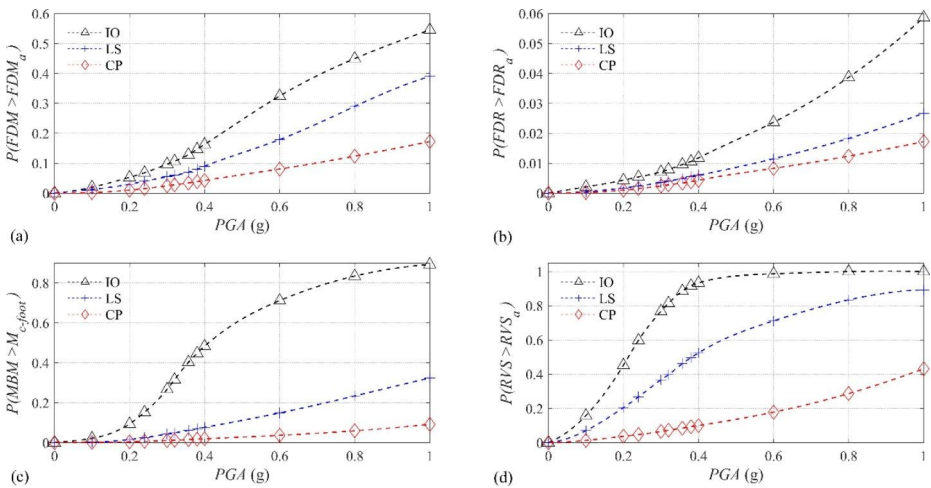

Fig. 14 Fragility curves for bridge pier with RSF corresponding to H_c/B_f = 3.0 for four EDPs and pulse-type earthquakes: (a) *FDM*; (b) *FDR*; (c) *MBM*; and (d) *RVS*

the values of the *FDR* is negligible due to recentering of the bridge pier-RSF system after the earthquake event.

4 Conclusions

The fragility analysis of the bridge pier-RSF system is performed to quantify the seismic damage in a probabilistic framework in the paper. For the response analysis of the system,

Fig. 15 Comparison of P_f values of four EDPs with PGA for $H_c/B_f = 2.5$: LS performance level for broadband and pulse-type motions
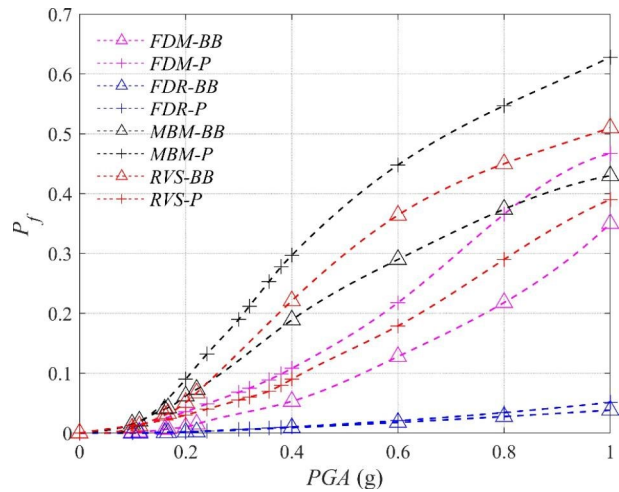
five broadband-type and five pulse-type ground motions are selected from the PEER ground motion database such that the mean spectrum of these motions is compatible with the target response spectrum of IS 1893 (Part 1): 2016 for Zone IV and Type II soil. These ten ground motions are scaled to generate sixty more ground motions to reflect the amplitudes corresponding to the no failure state to the certain failure of the bridge pier-RSF system. The probabilities of failure are evaluated using the MCS technique with LHS. The fragility curves are developed considering the four EDPs (i.e., *FDM*, *FDR*, *MBM* and *RVS*), four model configurations (H_c/B_f ratios of 1.5, 2, 2.5, and 3) and three performance levels (IO, LS and CP). The developed fragility curves can be used to assess the probable damage state of the bridge pier with RSF under different PGA and accordingly the loss estimates and retrofitting strategies can be undertaken. The following conclusions are made based on the results of this study.

- The rocking of the foundation increases with decrease in the width of the foundation. The maximum bending moment of the footing and horizontal displacement of the deck due to flexure alone decrease with decrease in the width of the footing whereas the residual vertical settlement shows the opposite trend. Therefore, one should be careful while dimensioning the RSF in the design of bridges. It is advised to dimension the RSF based on the required performance expected out of the structure and specify the performance criterion as a combination of the performance level and maximum probability of exceedance.
- The developed fragility curves show that the bridge pier-RSF system is more vulnerable in the case of pulse-type ground motions compared to the broadband-type ground motions. However, even in the case of pulse-type ground motions, the beneficial effects of the RSF are still significant.
- The values of the probability of failure for residual horizontal displacement of the deck due to flexure is found to be very small compared to the residual vertical settlement for both the pulse and broadband-type ground motions. The results of the study emphasize the fact that, even though the bridge pier-RSF system may undergo larger settlements

during an earthquake event, it remains structurally stable owing to recentering of the system post the seismic activity.

Author contributions All authors contributed to the study conception and design. Material preparation, data collection and analysis were performed by [B S Deviprasad]. The first draft of the manuscript was written by [B S Deviprasad] and all authors commented on previous versions of the manuscript. All authors read and approved the final manuscript.

Data Availability The datasets generated during and/or analyzed during the current study are available from the corresponding author on reasonable request.

Declarations

Competing Interests The authors declare that they have no known competing financial interests or personal relationships that could have appeared to influence the work reported in this paper.

References

Anastasopoulos I, Gazetas G, Loli M, Apostolou M, Gerolymos N (2010) Soil failure can be used for seismic protection of structures. Bull Earthq Eng 8(2):309–326. https://doi.org/10.1007/s10518-009-9145-2

Antonellis G (2015) Numerical and Experimental Investigation of Bridges with Columns Supported on Rocking Foundations. Ph.D. Thesis, University of California, Berkeley, USA

Boulanger RW, Curras CJ, Kutter BL, Wilson DW, Abghari A (1999) Seismic soil-pile-structure interaction experiments and analyses. J Geotech Geoenvironmental Eng ASCE 125(9):750–759. https://doi.org/10.1061/(ASCE)1090-0241(1999)125:9(750)

Boulanger RW (2000) The PySimple1, QzSimple1, and TzSimple1 material documentation, Document for the OpenSees platform, http://opensees.berkeley.edu

Bozozuk L (1978) Bridge Foundation Move. Transportation Research Record No. 678, Transportation Research Board, Washington, DC, 17–21

Deng L, Kutter BL, Kunnath SK (2012) Centrifuge modeling of bridge systems designed for rocking foundations. J Geotech GeoEnviron Eng 138(3):335–344. https://doi.org/10.1061/(ASCE)GT.1943-5606.0000605

Deng L, Kutter BL (2012) Characterization of rocking shallow foundations using centrifuge model tests. Earthquake Eng Struct Dynam 41:1043–1060

Deviprasad BS, Dodagoudar GR (2020) Seismic response of bridge pier supported on rocking shallow foundation. Geomech Eng 21(1):73–84. https://doi.org/10.12989/gae.2020.21.1.073

Deviprasad BS, Saseendran R, Dodagoudar GR (2021) Reliability Analysis of Bridge Pier Supported on Rocking Shallow Foundation Under Earthquake Loading. Int J Geomech ASCE. https://doi.org/10.1061/(ASCE)GM.1943-5622.0002287

Díaz SA, Pujades LG, Barbat AH, Hidalgo-Leiva DA, Vargus-Alzate YF (2018) Capacity, damage and fragility models for steel buildings: a probabilistic approach. Bull Earthq Eng 16:1209–1243. https://doi.org/10.1007/s10518-017-0237-0

Elnashai A, Borzi B, Vlachos S (2004) Deformation-based vulnerability functions for RC bridges. Struct Eng Mech 17(2):215–244

EC8 (2003) Design of structures for Earthquake Engineering Resistance, Part 3: Strengthening and Repair of Buildings, EN, 1998–3 European Committee for Standardization, Brussels

FEMA 356 (2000) Prestandard and commentary for the seismic rehabilitation of buildings. Federal Emergency Management Agency, Washington DC

Gerolymos N, Giannakou A, Anastasopoulos I, Gazetas G (2008) Evidence of beneficial role of inclined piles: observations and numerical results. Bull Earthq Eng 6(4):705–722 Special Issue: Integrated approach to fault rupture- and soil-foundation interaction

Gerolymos N, Drosos V, Gazetas G(2009) Seismic response of single-column bent on pile: evidence of beneficial role of pile and soil inelasticity. Bulletin of Earthquake Engineering 7(2), 547–573, Special Issue: Earthquake Protection of Bridges, https://doi.org/10.1007/s10518-009-9111-z

Giordano N, De Luca F, Sextos A (2021) Analytical fragility curves for masonry school building portfolios in Nepal. Bull Earthq Eng 19:1121–1150. https://doi.org/10.1007/s10518-020-00989-8

Herdrich B(2015) Parametric study of rocking shallow foundations under seismic excitation. M.S project report, Portland state university, Portland, USA

Hwang H, Jernigan J, Lin Y (2000) Evaluation of seismic damage to Memphis bridges and highway systems. J Bridge Eng ASCE 5(4):322–330

IS 1893 (2016) Criteria for Earthquake Resistant Design of Structures, Part 1: General Provisions and Buildings. Bureau of Indian Standards, New Delhi

Jeong S, Elnashai A (2007) Probabilistic fragility analysis parameterized by fundamental response quantities. Eng Struct 29(6):1238–1251

Kim SH, Feng MQ (2003) Fragility analysis of bridges under ground motion with spatial variation. Int J Non-Linear Mech 38:705–721. https://doi.org/10.1016/S0020-7462(01)00128-7

Kutter BL, Martin GR, Hutchinson T, Harden C, Gajan S, Phalen J (2006) Workshop on modeling of nonlinear cyclic load-deformation behavior of shallow foundations. PEER workshop Report No. 2005/14. University of California Berkeley, USA

Liu LL, Cheng YM (2020) System reliability analysis of soil slopes using an advanced kriging metamodel and quasi–Monte Carlo Simulation. Int J Geomech ASCE 06018019. https://doi.org/10.1061/(ASCE)GM.1943-5622.0001209

Mackie KR, Stojadinovic B (2005) Fragility basis for California Highway Overpass Bridge Seismic Decision Making. PEER, Report 2005/02. University of California Berkeley, USA

Ni P, Mangalathu S, Liu K (2020) Enhanced fragility analysis of buried pipelines through lasso regression. Acta Geotech 15(2):471–487. https://doi.org/10.1007/s11440-018-0719-5

Ni P, Mangalathu S, Yi Y (2018) Fragility analysis of continuous pipelines subjected to transverse permanent ground deformation. Soils Found 58(6):1400–1413. https://doi.org/10.1016/j.sandf.2018.08.002

Nielson BG(2005) Analytical Fragility Curves for Highway Bridges in Moderate Seismic Zones. Ph.D. Thesis, Georgia Institute of Technology, Atlanta, Georgia

Paolucci R (1997) Simplified evaluation of earthquake-induced permanent displacement of shallow foundations. J Earthquake Eng 1(3):563–579. https://doi.org/10.1080/13632469708962378

Pecker A(2003) Aseismic foundation design process, lessons learned from two major projects: the Vascode Gama and the Rion Antirion bridges. ACI International Conference on Seismic Bridge Design and Retrofit, University of California, San Diego, USA

Pelekis I, McKenna F, Madabhushi GSP (2021) Finite element modeling of buildings with structural and foundation rocking on dry sand. Earthquake Eng Struct Dynam 50(12):3093–3115. https://doi.org/10.1002/eqe.3501

Radu A, Grigoriu M (2018) An earthquake-source-based metric for seismic fragility analysis. Bull Earthq Eng 16:3771–3789. https://doi.org/10.1007/s10518-018-0341-9

Raychowdhury P(2008) Nonlinear Winkler-based shallow foundation model for performance assessment of seismically loaded structures. Ph.D Thesis, University of California, San Diego, USA

SDC 1.6 (2010) Caltrans Seismic Design Criteria version 1.6. California Department of Transportation, Sacramento, California

Shinozuka M, Feng M, Lee J, Naganuma T (2000) Statistical Analysis of Fragility Curves. J Eng Mech ASCE 126(12):1224–1231

Yakut A, Solmaz T(2012) Performance based displacement limits for reinforced concrete columns under flexure. 15th World Conference on Earthquake Engineering, Lisbon, Portugal, 2012